

Abstract

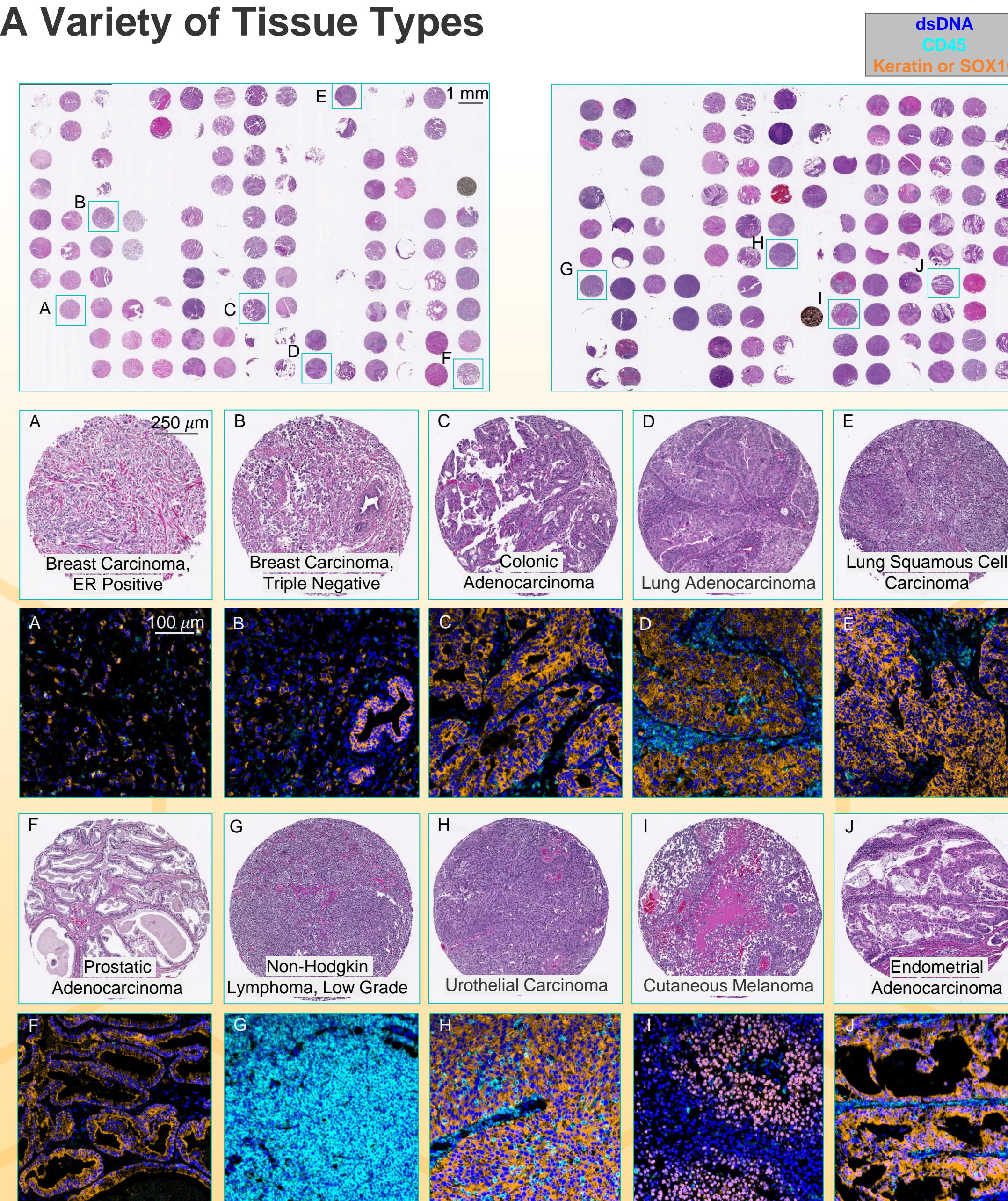
Background: An ability to characterize the cellular composition and spatial organization of the TME using multiplexed IHC has been limited by the techniques available. Here we show the applicability of MIBI™ technology for cell phenotype identification and spatial relationships analysis across multiple tumor types.

Methods: FFPE samples from tumor TMAs were stained with a panel of 15 antibodies, each labeled with a specific metal isotope. Brightfield IHC served as a comparator to establish that the labeling procedure did not affect antibody affinity. In MIBI the stained section was scanned via secondary ion mass spectrometry to image the tissue for target expression. Leave-one-out (LOO) analyses (a single antibody left out of the panel, compared to the full MIBI panel) showed negligible loss in signal intensity of targets indicating an absence of interference between antibodies. Multi-step processing and segmentation produced images of the TME and the frequency of different cell subsets. Distances between cell subsets were calculated using this data.

Results: Panel validation by LOO showed that all markers were repeatable across 9 panels (R^2 0.94 - 1.00). Control samples imaged at study start and end showed consistent marker quantification (inter-run $R^2 > 0.99$), indicating MIBI staining and acquisition is robust and reproducible. A total of 50 tumor specimens from 15 tumor types were characterized for their immune profile and spatial organization (nearest-neighbor). Most samples showed infiltrating cytotoxic T cells and macrophages present amongst tumor cells. Spatial analysis of the TME in two ovarian serous carcinoma samples showed differences in the distance between tumor and immune cells, highlighting the degree of mixing between tumor and immune cells. Identification of admixed PD-L1⁺ macrophages and PD-1⁺ T cells in a urothelial carcinoma sample allowed for calculation of distances to each other.

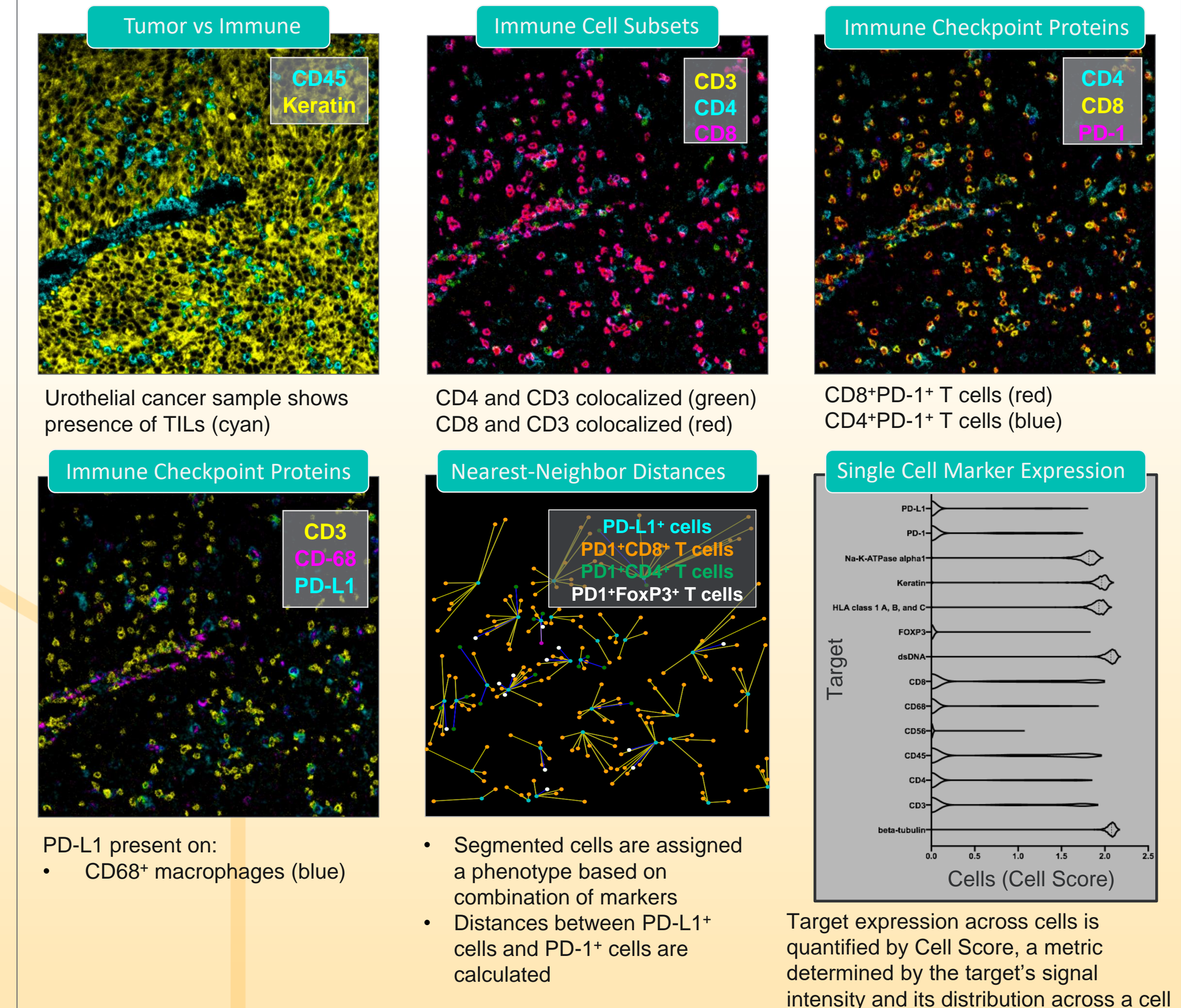
Conclusions: MIBI offers high-parameter multiplexing capability, at sensitivity and resolution uniquely suited to understanding the complex tumor immune landscape including the spatial relationship of immune and tumor cells and expression of immunoregulatory proteins.

MIBI Data Recapitulates IHC Staining Patterns Across A Variety of Tissue Types



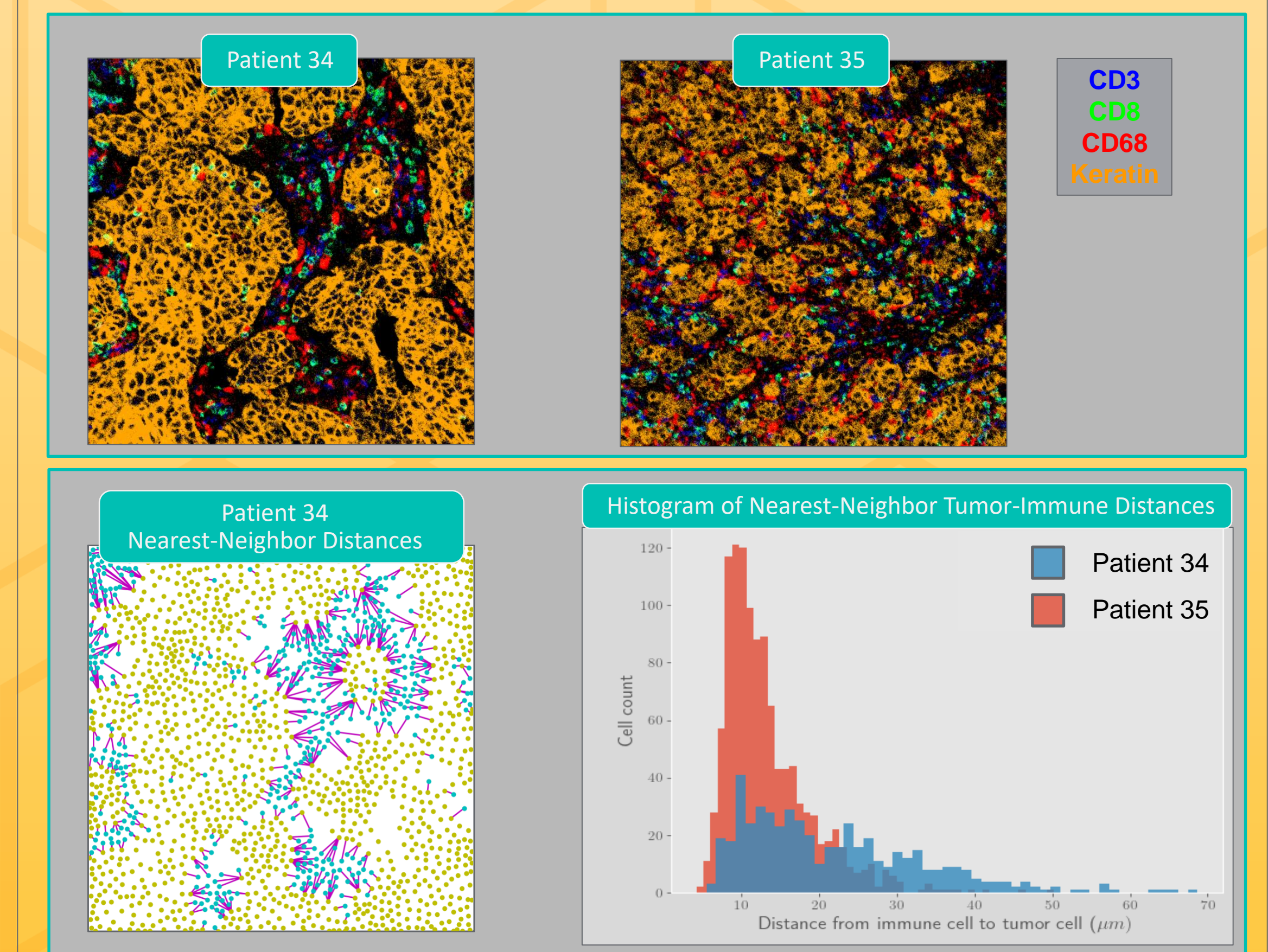
- Example images of 10 tumor types comparing H&E images to MIBI.
- MIBI images showing a subset of markers analyzed by MIBI illustrate the spatial organization of tumor cells and immune cells.

Single Cell Profiling of Immune Subsets of the TME



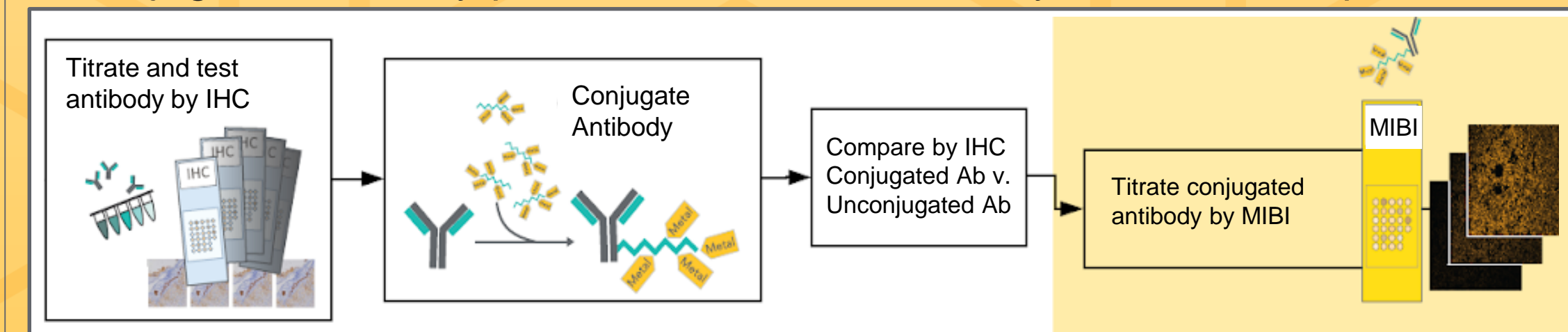
Spatial Distribution of Immune Cells and Tumor Cells Differs Between Ovarian Cancer Samples

- Patient 34 shows a compartmentalized organization of the TME versus Patient 35 that shows mixing of immune cells and tumor cells.
- Calculation of nearest-neighbor distances between tumor cells and the nearest immune cells further characterizes differences in TMEs.

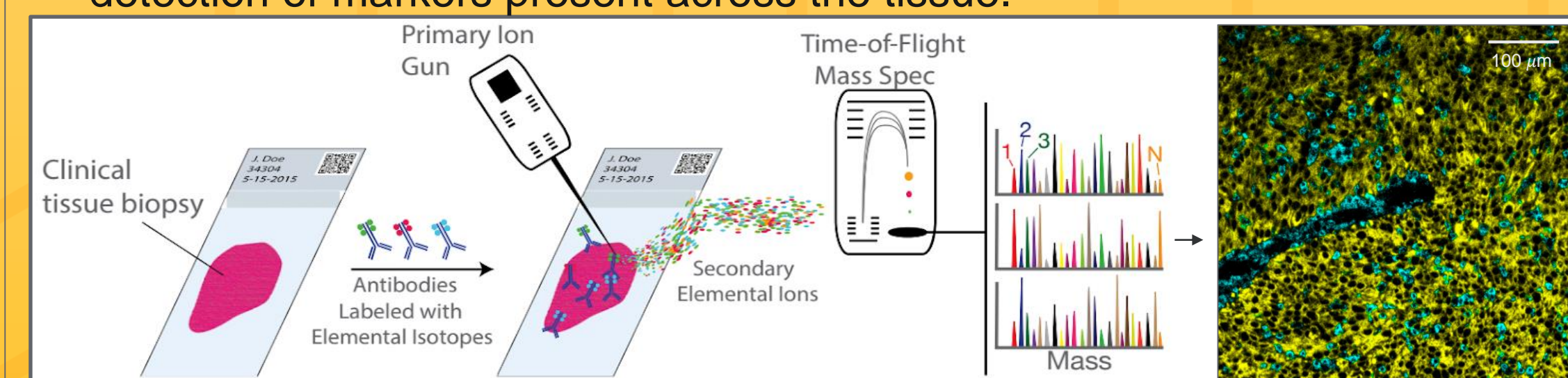


Multiplexed Ion Beam Imaging (MIBI)

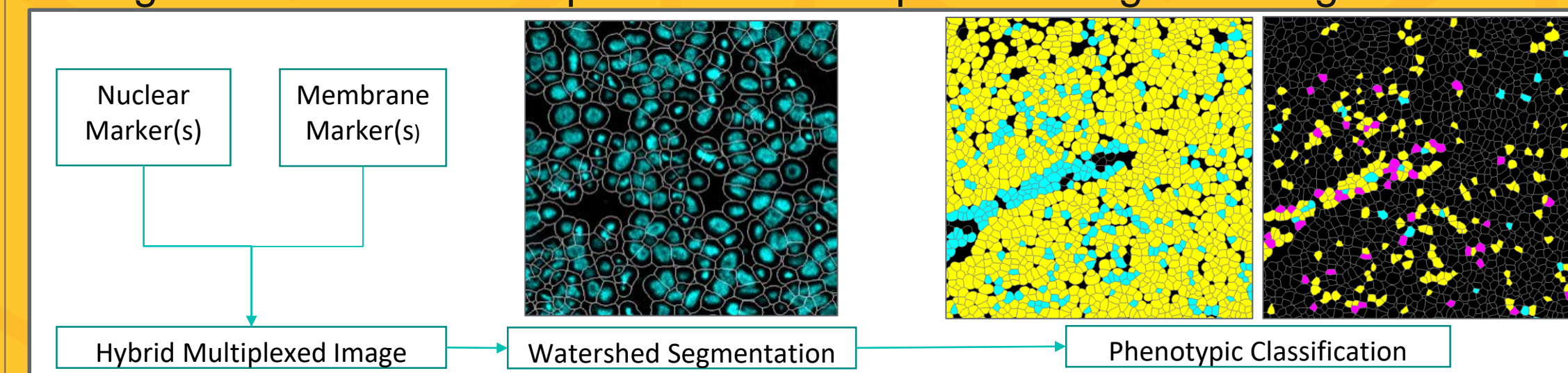
- Antibody performance is assessed by IHC before conjugation to an isotope.
- Conjugated antibody performance is measured by MIBI and compared to IHC.



- An ion beam rasters across the tissue liberating ions including the isotopes bound to the tissue via the antibodies.
- Time-of-flight mass spectrometry separates the labels based on mass for detection of markers present across the tissue.



- MIBI preserves spatial information allowing tumor-immune cell boundary and distance determination.
- Segmentation uses multiplexed data and prior training data as ground truth.



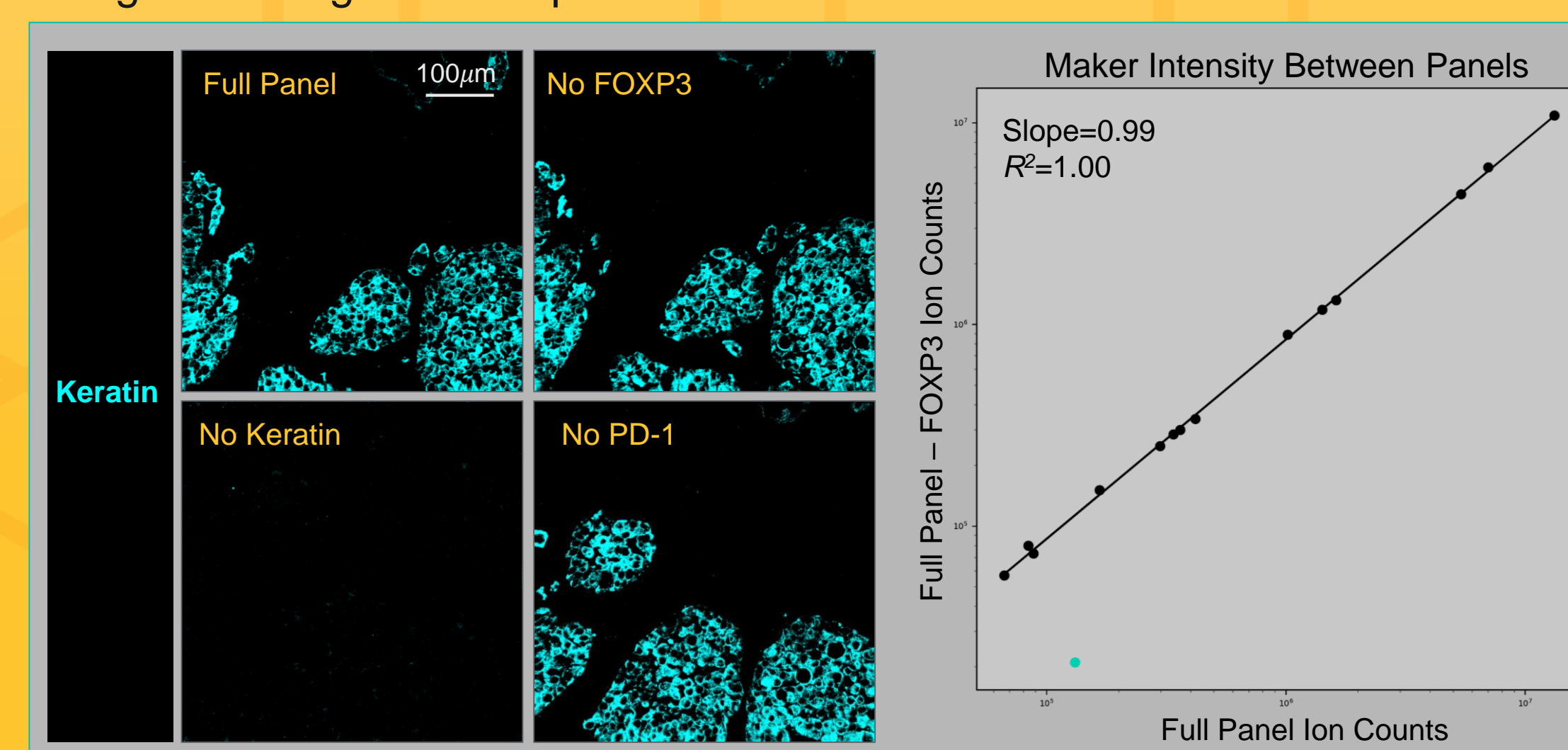
Staining Panel For Phenotypic Analysis of the TME

Target	Clone	Label	Cell Expression
dsDNA	3519 DNA	89Y	All cells
beta-tubulin	D3U1W	166Er	All cells
HLA class 1 A, B, and C	EMR8-5	160Gd	All cells
Na-K ATPase alpha1	D4Y7E	176Yb	All cells
Keratin	AE1/AE3	165Ho	Tumor cells, epithelial cells
CD3	D7A6E	159Tb	T cells
CD4	EPR6855	143Nd	T helper cells, some macrophages
CD8	C8/144B	158Gd	Cytotoxic T cells
CD45	2B11 & PD7/26	175Lu	Immune cells
CD56	MRQ-42	150Nd	NK cells, neurons
CD68	D4B9C	156Gd	Macrophages
FOXP3	236A/E7	146Nd	Regulatory T cells
PD-1	D4W2J	148Nd	T cells
PD-L1	E1L3N	149Sm	Tumor cells, macrophages, APCs
SOX10	BC34	170Er	Melanocytes, nerve cells

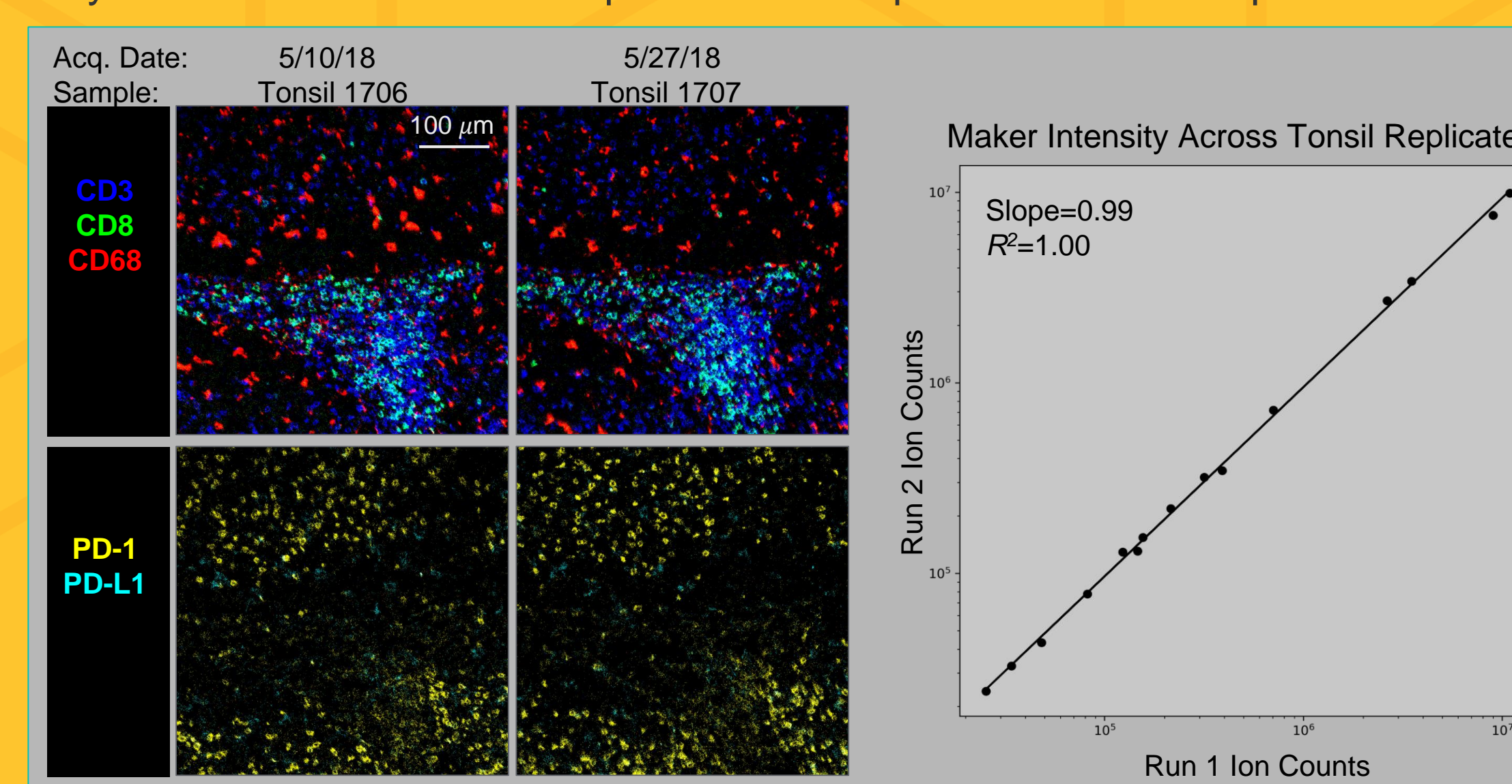
MIBI Data Reproducible For High, Medium and Low Abundance Targets

- Serial sections of lung adenocarcinoma were stained with either the full panel or panels that lacked one antibody (LOO panel).
- Regression analysis of signal intensity between Full and LOO panels are summarized in the table.
- Images of keratin expression are similar between the full panel and panels lacking FOXP3 or PD-1.
- Keratin signal is absent from the TMA stained with the panel without keratin demonstrating the lack of significant signal overlap across channels.

LOO Panel	R^2
Full - FOXP3	1.00
Full - PD-1	1.00
Full - PD-L1	1.00
Full - CD56	0.99
Full - CD68	1.00
Full - CD8	1.00
Full - Keratin	0.99
Full - Sox10	0.99



- Replicate serial sections of tonsil (shown), placenta, and melanoma acquired by MIBI before and after acquisition of sample cohort show equivalent results.



Conclusions

- MIBI offers many features advantageous for the analysis of complex tissues including the tumor microenvironment.
- MIBI control data indicates that staining and sample acquisition is robust and repeatable across tissue types.
- The tissue architecture is defined at sub-cellular resolution enabling segmentation that further enables single-cell analysis and phenotypic characterization.
- Sensitivity afforded from the low background of MIBI allows for markers with low expression such as PD-1 and FOXP3 to be readily detected.
- This study evaluating multiple tumor types shows the possibilities of MIBI for patient stratification and immune profiling of tumor samples under therapeutic forces.

Acknowledgements

We thank all patients who have donated samples for this investigation.